

# Interaction between two modes of a field mediated by two quantum dots in a photonic crystal cavity

J. K. Verma <sup>1</sup>, Harmanpreet Singh <sup>1</sup>, P. K. Pathak <sup>1</sup>, and S. Hughes <sup>2</sup>  
<sup>1</sup>*Indian Institute of Technology Mandi, Mandi 175 001, Himachal Pradesh, India*  
<sup>2</sup>*Department of Physics, Queen's University, Kingston, ON K7L 3N6, Canada*

(Dated: March 11, 2020)

We show unusual cooperative two-photon resonance between two-modes of a field inside a photonic crystal cavity. The cooperative two-mode two-photon resonance occurs when two off-resonant quantum dots emit one photon in each cavity mode and de-excite simultaneously. Using such two-photon two-mode interaction we propose to generate an entangled state of two qutrits. The bases for the qutrits are formed by the states of the cavity modes containing 0, 1 and 2 photons. We also discuss the effect of phonon coupling on the entanglement and the probability of generating two-qutrit state.

PACS numbers: 03.65.Ud, 03.67.Mn, 42.50.Dv

## I. INTRODUCTION

Semiconductor quantum dots (QDs) embedded in a photonic crystal cavity have emerged as a new paradigm in cavity quantum electrodynamics<sup>1</sup>. These on-chip systems have been extensively explored theoretically and experimentally in the last two decades, particularly, in the quest of scalable quantum optical technology<sup>2</sup>. Various quantum optical phenomena such as enhanced exciton decay rate<sup>3</sup>, vacuum Rabi splitting<sup>4</sup>, Rabi oscillations<sup>5</sup>, Mollow triplets have been observed<sup>6</sup>. The sources of nonclassical light such as entangled photons<sup>7-10</sup> and indistinguishable single photons<sup>11</sup> have also been realized successfully. Analogous to electrons in atoms, excitons in QDs have discrete energy levels. However, QDs are semiconductor material therefore exciton-phonon interactions are inevitable<sup>12,13</sup>. In a typical experiment, a QD embedded in the photonic crystal cavity is excited by an external field incoherently<sup>14</sup> or by using recently developed coherent pumping methods<sup>15</sup> and the fluorescence is detected. Signatures of phonon interaction in QDs have been observed first in the systems using incoherent pumping which result in exciton dephasing and cavity mode feeding in off-resonant QD cavity interaction<sup>16</sup>. In incoherently pumped QDs, phonon-induced off-resonant interactions with charged excitons generated during pumping and wetting-layer continuum states have been found responsible for these phenomena<sup>17</sup>. Using a coherent pump, the problems such as transitions from charged excitons and wetting-layer do not contribute significantly and only the exciton-phonon coupling remains relevant. Further, phonon interactions become more prominent in off-resonant interaction between QD and electromagnetic fields. Therefore, off-resonant QD-cavity QED provides a platform for studying interaction between exciton, photon, and phonon together<sup>6,18-21</sup>. Various new phonon-assisted phenomena in off-resonant QDs have also been observed, recently. For example, exciton and biexciton states can be prepared with high fidelity<sup>22</sup>, using off-resonant pumping field, in the presence of phonon interaction. For generating exciton state the laser pulse is tuned above the exciton resonance and for biexciton state preparation laser is tuned resonant to exciton transition making exciton to biexciton transition off-resonant by the binding energy of the biexciton. The population inversion which can not be achieved in two-level systems has been demonstrated in two-level QDs due to exciton-phonon coupling when the pump field is tuned above the exciton resonance<sup>23</sup>. Fast control of QD laser emission has also been demonstrated using acoustic pulses<sup>24</sup>. Various new features due to phonon interactions have been observed in the Mollow triplet for off-resonant QD-cavity system<sup>6</sup>. All these studies have been done using single QDs. Recently, Majumdar et al have observed excitation transfer between two QDs embedded inside a photonic crystal cavity<sup>18</sup>. In our earlier work, we have also predicted that phonon induced two-photon interaction between two off-resonant QDs<sup>20</sup> interacting with a single mode field could be very large. In this work, we show that exciton-phonon interaction in off-resonant QDs in a bimodal cavity can lead to unusual two-photon resonant interaction between two cavity modes. We also predict that such interaction can be exploited in generating entangled state of two photons, emitted through two modes, of the form  $|\psi\rangle \sim (|0, 2\rangle + |1, 1\rangle + |2, 0\rangle)/\sqrt{3}$ . A lot of work has been done for generating entangled state of two photons of the form  $|\phi\rangle \sim (|x_1, x_2\rangle + |y_1, y_2\rangle)/\sqrt{2}$ , in a bimodal cavity through biexciton cascaded decay<sup>21,25,26</sup>. Here 1, 2 represent two modes in frequency and  $x, y$  represent two orthogonal polarizations. Here, we show the phonon-assisted generation of entangled qutrit states of two photons emitted from two cavity modes.

Our paper is organized as follows. In Sec.II, we present our model for resonant two-photon interaction between two modes and develop theoretical formalism using recently developed master equation techniques<sup>27</sup>. We discuss two-photon two-mode resonant interaction using population dynamics, probabilities for photon emissions, and spectrum of the generated photons in Sec.III. We discuss entanglement between two modes in terms of negativity and show its

dependence on temperature in Sec.IV. Finally, we present conclusions in Sec.V.

## II. POLARON TRANSFORMED MASTER EQUATION FOR TWO QDS IN A BIMODAL CAVITY

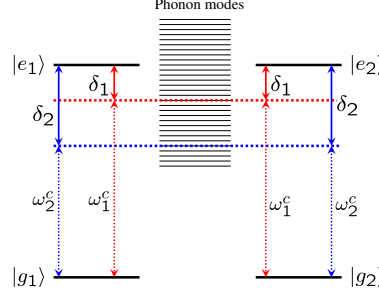


FIG. 1: (Color online) The schematic energy level diagram for two separated QDs interacting with two modes of a field inside a photonic crystal cavity.

We consider two separated QDs interacting off-resonantly with two modes of a field inside a photonic crystal cavity as shown in Fig.1. We also consider exciton resonance frequencies are same in both QDs and are equal to  $\omega_0$ . The Hamiltonian in the rotating frame with exciton resonance frequency is given by

$$H = -\hbar\delta_1 a_1^\dagger a_1 - \hbar\delta_2 a_2^\dagger a_2 + \hbar \sum_{i=1,2} (g_i \sigma_i^+ a_i + g'_i \sigma_2^+ a_i + H.c.) + H_{ph}. \quad (1)$$

Here  $\delta_i = \omega_0 - \omega_i^c$  is detuning between exciton resonance and cavity mode of frequency  $\omega_i^c$ ,  $g_i$  and  $g'_i$  are dipole coupling constants of first and second QDs with  $i$ th cavity mode,  $\sigma_i^+ = |e_i\rangle\langle g_i| = (\sigma_i^-)^\dagger$  is exciton creation operator in  $i$ th QD and  $a_i$  is photon annihilation operator in  $i$ th cavity mode. We notice that a similar Hamiltonian for single QD interacting with two modes has been realized in an experiment to demonstrate photon blockade<sup>28</sup> in QD-cavity system. A single QD has been coupled to both horizontally and vertically polarized cavity modes due to orientation mismatch of its dipole by angle  $\theta$ . The coupling constants with cavity modes have the form  $g_1 = g \cos \theta$  and  $g_2 = g \sin \theta$ . The longitudinal acoustic phonon bath and exciton-phonon interactions are included in  $H_{ph} = \hbar \sum_k \omega_k b_k^\dagger b_k + \lambda_k \sigma_1^+ \sigma_1^- (b_k + b_k^\dagger) + \mu_k \sigma_2^+ \sigma_2^- (b_k + b_k^\dagger)$ ; where  $\lambda_k, \mu_k$  are exciton phonon coupling constants and  $b_k, b_k^\dagger$  are annihilation, creation operators for  $k$ th phonon mode of frequency  $\omega_k$ . In order to keep exciton-phonon coupling up to all order we use polaron transformed Hamiltonian. The transformed Hamiltonian  $H' = e^P H e^{-P}$  with  $P = \sigma_1^+ \sigma_1^- \sum_k \frac{\lambda_k}{\omega_k} (b_k - b_k^\dagger) + \sigma_2^+ \sigma_2^- \sum_k \frac{\mu_k}{\omega_k} (b_k - b_k^\dagger)$ ; can be written as the sum of terms corresponding to cavity-QD system, phonon bath and system-bath interactions as  $H' = H_s + H_b + H_{sb}$ , where

$$H_s = -\hbar\Delta_1 a_1^\dagger a_1 - \hbar\Delta_2 a_2^\dagger a_2 + \langle B \rangle X_g, \quad (2)$$

$$H_b = \hbar \sum_k \omega_k b_k^\dagger b_k, \quad (3)$$

$$H_{sb} = \xi_g X_g + \xi_u X_u. \quad (4)$$

The polaron shifts  $\sum_k \lambda_k^2 / \omega_k, \sum_k \mu_k^2 / \omega_k$  are included in the effective detunings  $\Delta_1$  and  $\Delta_2$ . The system operators are given by  $X_g = \hbar \sum_{j=1,2} (g_j \sigma_1^+ a_j + g'_j \sigma_2^+ a_j) + H.c.$ ,  $X_u = i\hbar \sum_{j=1,2} (g_j \sigma_1^+ a_j + g'_j \sigma_2^+ a_j) + H.c.$  and the phonon field fluctuation operators are  $\xi_g = \frac{1}{2}(B_+ + B_- - 2\langle B \rangle)$  and  $\xi_u = \frac{1}{2i}(B_+ - B_-)$  where  $B_\pm = \exp[\pm \sum_k \frac{\lambda_k}{\omega_k} (b_k - b_k^\dagger)] = \exp[\pm \sum_k \frac{\mu_k}{\omega_k} (b_k - b_k^\dagger)]$  are phonon displacement operators with expectation value  $\langle B \rangle = \langle B_+ \rangle = \langle B_- \rangle$ . The multiplication by  $\langle B \rangle$  (which is smaller than 1 for finite temperature) in the system hamiltonian shows reduction in QD-cavity couplings in the presence of phonon interactions. We use transformed Hamiltonian  $H'$  and Born-Markov

approximation to derive polaron master equation for describing the dynamics of the system. The spontaneous emission, cavity damping and phonon induced dephasing are also included in Lindblad form. The Lindblad super operator corresponding to an operator  $\hat{O}$  is defined as  $\mathcal{L}[\hat{O}]\rho = \hat{O}^\dagger\hat{O}\rho - 2\hat{O}\rho\hat{O}^\dagger + \rho\hat{O}^\dagger\hat{O}$ . The final form of master equation in terms of reduced density matrix for cavity-QDs coupled system,  $\rho_s$ , is written as<sup>27</sup>

$$\begin{aligned} \dot{\rho}_s = & -\frac{i}{\hbar}[H_s, \rho_s] - \mathcal{L}_{ph}\rho_s \\ & - \sum_{i=1,2} \left( \frac{\kappa_i}{2}\mathcal{L}[a_i] + \frac{\gamma_i}{2}\mathcal{L}[\sigma_i^-] + \frac{\gamma'_i}{2}\mathcal{L}[\sigma_i^+\sigma_i^-] \right) \rho_s, \end{aligned} \quad (5)$$

where  $\kappa_i$  is photon leakage rate from  $i$ th cavity mode and  $\gamma_i, \gamma'_i$  are spontaneous decay, dephasing rates for  $i$ th QD, and

$$\mathcal{L}_{ph}\rho_s = \frac{1}{\hbar^2} \int_0^\infty d\tau \sum_{j=g,u} G_j(\tau) [X_j(t), X_j(t, \tau)\rho_s(t)] + H.c. \quad (6)$$

where  $X_j(t, \tau) = e^{-iH_s\tau/\hbar} X_j(t) e^{iH_s\tau/\hbar}$ , and  $G_g(\tau) = \langle B \rangle^2 \{ \cosh[\phi(\tau)] - 1 \}$  and  $G_u(\tau) = \langle B \rangle^2 \sinh[\phi(\tau)]$ . The phonon bath is treated as a continuum with spectral function  $J(\omega) = \alpha_p \omega^3 \exp[-\omega^2/2\omega_b^2]$ , where the parameters  $\alpha_p$  and  $\omega_b$  are the electron-phonon coupling and cutoff frequency respectively. In our calculations we use  $\alpha_p = 1.42 \times 10^{-3} g_1^2$  and  $\omega_b = 10g_1$ , which gives  $\langle B \rangle = 1.0, 0.90, 0.84,$  and  $0.73$  for  $T = 0K, T = 5K, 10K,$  and  $20K$ , respectively, these values match with recent experiments<sup>27,29</sup>. The system-phonon interactions are included in phonon correlation function  $\phi(\tau)$  given by

$$\phi(\tau) = \int_0^\infty d\omega \frac{J(\omega)}{\omega^2} \left[ \coth\left(\frac{\hbar\omega}{2K_b T}\right) \cos(\omega\tau) - i \sin(\omega\tau) \right], \quad (7)$$

where  $K_b$  and  $T$  are Boltzmann constant and the temperature of phonon bath respectively.

We are interested in two-photon cooperative interaction between two cavity modes, therefore we work in the condition when QDs are far off-resonant with cavity modes, i.e. the detunings between cavity modes and exciton resonance in QDs are much larger than their couplings ( $\Delta_1, \Delta_2 \gg g_i, g'_i$ ). Under such condition the master equation (5) can be further simplified, using  $H_s = -\hbar\Delta_1 a_1^\dagger a_1 - \hbar\Delta_2 a_2^\dagger a_2$ , after neglecting the terms proportional to  $g_i$  and  $g'_i$ , in the expression of  $X_j(t, \tau)$ . For simplification we also consider  $g_i = g'_i$ . After such approximation master equation takes the perfect Lindblad form which provides clear picture of different processes involved in the dynamics. The approximated Lindblad form of master equation (5) is given by

$$\begin{aligned} \dot{\rho}_s = & -\frac{i}{\hbar}[H_{eff}, \rho_s] \\ & - \sum_{i=1}^2 \left( \frac{\kappa_i}{2}\mathcal{L}[a_i] + \frac{\gamma_i}{2}\mathcal{L}[\sigma_i^-] + \frac{\gamma'_i}{2}\mathcal{L}[\sigma_i^+\sigma_i^-] \right) \rho_s \\ & - \sum_{i,j,k,l=1, i \neq j}^2 \frac{\Gamma_{kl}^{--}}{2} (a_l^\dagger \sigma_j^- a_k^\dagger \sigma_i^- \rho_s - 2a_k^\dagger \sigma_i^- \rho_s a_l^\dagger \sigma_j^- + \rho_s a_l^\dagger \sigma_j^- a_k^\dagger \sigma_i^-) \\ & - \sum_{i,j,k,l=1, i \neq j}^2 \frac{\Gamma_{kl}^{++}}{2} (\sigma_j^+ a_l \sigma_i^+ a_k \rho_s - 2\sigma_i^+ a_k \rho_s \sigma_j^+ a_l + \rho_s \sigma_j^+ a_l \sigma_i^+ a_k) \\ & - \sum_{i,j,k,l=1}^2 \frac{\Gamma_{kl}^{+-}}{2} (a_l^\dagger \sigma_j^- \sigma_i^+ a_k \rho_s - 2\sigma_i^+ a_k \rho_s a_l^\dagger \sigma_j^- + \rho_s a_l^\dagger \sigma_j^- \sigma_i^+ a_k) \\ & - \sum_{i,j,k,l=1}^2 \frac{\Gamma_{kl}^{-+}}{2} (\sigma_j^+ a_l a_k^\dagger \sigma_i^- \rho_s - 2a_k^\dagger \sigma_i^- \rho_s \sigma_j^+ a_l + \rho_s \sigma_j^+ a_l a_k^\dagger \sigma_i^-), \end{aligned} \quad (8)$$

where first term represents effective interaction between QDs and cavity field, second term represents leakage from cavity modes, spontaneous decays, and pure dephasing processes, and the other terms represent phonon induced

cavity-QD interactions. The effective Hamiltonian is given by

$$H_{eff} = H_s - i\hbar \sum_{i,j,k,l=1}^2 \Omega_{kl}^{+-} a_l^\dagger \sigma_j^- \sigma_i^+ a_k + \Omega_{kl}^{-+} \sigma_j^+ a_l a_k^\dagger \sigma_i^- - i\hbar \sum_{i,j,k,l=1, i \neq j}^2 \left( \Omega_{kl}^{--} a_l^\dagger \sigma_j^- a_k^\dagger \sigma_i^- + H.c. \right) \quad (9)$$

The terms containing  $\Omega_{kl}^{+-}$  and  $\Omega_{kl}^{-+}$  are corresponding to Stark shifts (for  $i = j$ ,  $k = l$ ), excitation transfer between QDs (for  $i \neq j$ ) and photon transfer between cavity modes (for  $k \neq l$ ). The last term for  $k = l$  represent cooperative two-photon interaction between two QDs and one cavity mode, and for  $k \neq l$  represents unusual cooperative interaction between two QDs and two cavity modes. The coupling constants for these processes are given by

$$\Omega_{kl}^{\pm\mp} = \frac{g_k g_l}{2} \int_0^\infty d\tau (G_+ e^{\pm i\Delta_k \tau} - G_+^* e^{\mp i\Delta_l \tau}) \quad (10)$$

$$\Omega_{kl}^{--} = \frac{g_k g_l}{2} \int_0^\infty d\tau (G_- e^{-i\Delta_k \tau} - G_-^* e^{-i\Delta_l \tau}), \quad (11)$$

with  $G_\pm = \langle B \rangle^2 (e^{\pm \phi(\tau)} - 1)$ . The rate of phonon assisted excitation transfer between QDs and photon transfer between two modes,  $\Gamma_{kl}^{\pm\mp}$ , and phonon induced two photon processes,  $\Gamma_{kl}^{\pm\pm}$ , are given by

$$\Gamma_{kl}^{\pm\mp} = g_k g_l \int_0^\infty d\tau (G_+ e^{\pm i\Delta_k \tau} + G_+^* e^{\mp i\Delta_l \tau}) \quad (12)$$

$$\Gamma_{kl}^{\pm\pm} = g_k g_l \int_0^\infty d\tau (G_- e^{\pm i\Delta_k \tau} + G_-^* e^{\pm i\Delta_l \tau}). \quad (13)$$

We solve master equation (5) numerically using quantum optics toolbox<sup>30</sup>. For large detunings, the results obtained from approximate Lindblad form of master equation (8) and the polaron master equation (5) match very well.

### III. COOPERATIVE TWO-MODE TWO-PHOTON INTERACTION

In order to reveal phonon induced two-photon interaction between two cavity modes, we consider QDs are off-resonantly coupled with cavity modes. In off-resonantly coupled QD-cavity systems the exciton-phonon interactions play vital role. In Figs.2 and 3, we consider different coupling strengths with cavity modes  $g_1 \neq g_2$ , while in Figs.4 and 5 we consider  $g_1 = g_2$ . Initially the QD-cavity system is in state  $|e_1, e_2, 0, 0\rangle$ , i.e. both QDs are in exciton state and there are no photons in the cavity modes. We plot photon emission probabilities,  $P_{10} = \kappa_1 \int_0^\infty \langle g_1, e_2, 1, 0 | \rho_s(t') | g_1, e_2, 1, 0 \rangle dt'$  from state  $|g_1, e_2, 1, 0\rangle$ ,  $P_{01} = \kappa_2 \int_0^\infty \langle g_1, e_2, 0, 1 | \rho_s(t') | g_1, e_2, 0, 1 \rangle dt'$  from state  $|g_1, e_2, 0, 1\rangle$ , which are equal to the photon emission probabilities from states  $|e_1, g_2, 1, 0\rangle$  and  $|e_1, g_2, 0, 1\rangle$ , respectively. We also plot photon emission probabilities from two photon states  $P_{20} = 2\kappa_1 \int_0^\infty \langle g_1, g_2, 2, 0 | \rho_s(t') | g_1, g_2, 2, 0 \rangle dt'$ ,  $P_{02} = 2\kappa_2 \int_0^\infty \langle g_1, g_2, 0, 2 | \rho_s(t') | g_1, g_2, 0, 2 \rangle dt'$ , and  $P_{11} = (\kappa_1 + \kappa_2) \int_0^\infty \langle g_1, g_2, 1, 1 | \rho_s(t') | g_1, g_2, 1, 1 \rangle dt'$  from states  $|g_1, g_2, 2, 0\rangle$ ,  $|g_1, g_2, 0, 2\rangle$ , and  $|g_1, g_2, 1, 1\rangle$ . In Fig.2, we fix detuning of the first cavity mode from exciton resonances to  $\Delta_1 = -5g_1 \langle B \rangle$  and scan detuning of the second cavity mode,  $\Delta_2$ , for two-photon two-mode resonance. In subplot (a), when the phonon interactions are absent, the probability of photon emission  $P_{02}$  from state  $|g_1, g_2, 0, 2\rangle$  has almost symmetric bell shape, having a peak at  $\Delta_2 = 0$ , which reflects that when second mode is resonant with both QDs the cooperative emission in state  $|g_1, g_2, 0, 2\rangle$  is dominating, leading to hyperradiant<sup>31</sup> behavior in high quality cavity. For positive values of  $\Delta_2$ , probability  $P_{11}$  starts dominating and has a peak at  $\Delta_2 = 3.5g_1$  which indicates resonant two-mode cooperative transitions from state  $|e_1, e_2, 0, 0\rangle$  to  $|g_1, g_2, 1, 1\rangle$  where both excitons decay simultaneously after emitting one photon in each cavity mode. The resonance condition is given by  $\Delta_1 + \Delta_2 + 2g_1^2/\Delta_1 + 2g_2^2/\Delta_2 \approx 0$ , i.e. when sum of frequencies of cavity modes is equal to the sum of exciton frequencies including Stark shifts. The probability  $P_{20}$  (cyan line) remains negligible for all values of  $\Delta_2$  indicating weak transition to state  $|g_1, g_2, 2, 0\rangle$ . The photon emission probabilities  $P_{10}$  (red line) and  $P_{01}$  (blue line) from states  $|g_1, e_2, 1, 0\rangle$  and  $|g_1, e_2, 0, 1\rangle$  also remain low and show dips when two-photon transitions in cavity modes are dominating. In subplots (b), (c), and (d) we introduce coupling with phonon bath at temperatures  $T = 5K$ ,  $T = 10K$ , and  $T = 20K$  respectively. In the presence of phonon interaction the peak at  $\Delta_2 = 3.5g_1$  in probability  $P_{11}$ , corresponding to resonant two-mode two-photon interaction disappears, which is due to the fact that the transition paths  $|e_1, e_2, 0, 0\rangle \rightarrow |g_1, e_2, 1, 0\rangle \rightarrow |g_1, g_2, 1, 1\rangle$ ,  $|e_1, e_2, 0, 0\rangle \rightarrow |e_1, g_2, 1, 0\rangle \rightarrow |g_1, g_2, 1, 1\rangle$  and

$|e_1, e_2, 0, 0\rangle \rightarrow |g_1, e_2, 0, 1\rangle \rightarrow |g_1, g_2, 1, 1\rangle$ ,  $|e_1, e_2, 0, 0\rangle \rightarrow |e_1, g_2, 1, 0\rangle \rightarrow |g_1, g_2, 1, 1\rangle$  become distinguishable due to the frequency difference between phonons involved in facilitating these off-resonant transitions. As a result the constructive interference responsible for two-mode two-photon resonant interaction diminishes. However, the probability  $P_{02}$  dominates for positive values of detuning,  $\Delta_2$ , due to the enhanced two-photon interaction with second mode followed by phonon emission in bath at low temperature<sup>20</sup>. On increasing bath temperature, enhancement for two-photon interactions between single-mode two-QD and two-mode two-QD for negative values of  $\Delta_2$  also occurs. For  $\Delta_2 = \Delta_1$ , a tiny resonance peak appears in  $P_{11}$  where  $P_{02}$  and  $P_{20}$  follow a dip, showing phonon-induced resonant two-mode two-photon transition to state  $|g_1, g_2, 1, 1\rangle$ . The phonon-assisted two-photon transitions in single mode and in two-mode are not significantly large for negative detunings. The probabilities  $P_{10}$  (red line) and  $P_{01}$  (blue line) remain small indicating small emission probabilities from individual QDs. In Fig.3, we fix detuning from first cavity

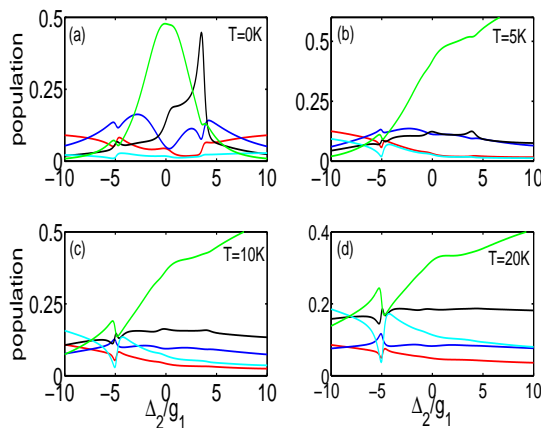


FIG. 2: Photon emission probabilities from the cavity modes,  $P_{10}$  from state  $|g_1, e_2, 1, 0\rangle$  (red line),  $P_{01}$  from state  $|g_1, e_2, 0, 1\rangle$  (blue line),  $P_{20}$  from state  $|g_1, g_2, 2, 0\rangle$  (cyan line),  $P_{02}$  from state  $|g_1, g_2, 0, 2\rangle$  (green line),  $P_{11}$  from state  $|g_1, g_2, 1, 1\rangle$  (black line). The parameters are  $g_2 = 1.5g_1$ ,  $\Delta_1 = -5g_1\langle B\rangle$ ,  $\kappa_1 = \kappa_2 = 0.1g_1$ ,  $\gamma_1 = \gamma_2 = \gamma'_1 = \gamma'_2 = 0.01g_1$ .

mode to positive value  $\Delta_1 = 5g_1\langle B\rangle$ . As expected, without phonon interaction, Fig.3(a) is mirror image of Fig.2(a). However, when the interaction with phonon bath is considered at  $T = 5K$  in Fig.3(b), the probability  $P_{20}$  dominates for negative values of  $\Delta_2$ . For positive values of  $\Delta_2 > 5g_1$ , the probability  $P_{02}$  dominates, indicating enhanced two photon transition in second mode. Further on increasing  $\Delta_2$  the probability  $P_{20}$  decreases and probabilities  $P_{11}$  and  $P_{02}$  increase. For  $\Delta_1 \approx \Delta_2$  probabilities  $P_{20}$  and  $P_{02}$  corresponding to two-photon transitions in individual cavity modes are equal and follow a minima whereas the probability  $P_{11}$  corresponding to phonon assisted cooperative two-mode two-photon transitions has a resonance peak. On increasing phonon bath temperature, in Fig.3(c) and (d), the two-photon transitions followed with phonon absorption are enhanced as a result the probabilities  $P_{02}$  and  $P_{11}$  increase for negative values of  $\Delta_2$ . The probabilities  $P_{10}$  and  $P_{01}$  corresponding to emission from individual QDs remain very small. It is clear that by changing detuning with the second cavity mode  $\Delta_2$  one can change the nature of the interaction of the first cavity mode. In Fig.4 and Fig.5, we consider equal dipole coupling strengths with both cavity modes  $g_1 = g_2$ , but  $\Delta_1 = -5g_1\langle B\rangle$  and  $\Delta_1 = 5g_1\langle B\rangle$ , respectively. It is clear from subplots Fig.4(a) and Fig.5(a), that in the absence of phonon interactions, the resonance peak in probability  $P_{11}$  corresponding to cavity induced two-mode two-photon interaction is negligible. In Fig.4(b), (c) and (d), the probability  $P_{02}$  has a peak at  $\Delta_2 = 0$  corresponding to hyperradiant behavior and dominates for positive values of  $\Delta_2$  indicating phonon assisted off-resonant interactions contribute significantly for positive detuning. Further, in Fig.4(b), (c) and (d), when temperature of phonon bath increases from 5K to 20K the probabilities  $P_{11}$  and  $P_{20}$  increases. There is a small resonance peak in  $P_{11}$  at  $\Delta_2 = \Delta_1$  corresponding to phonon induced two-mode two-photon resonance which grows on increasing temperature as phonon absorption probability increases. However the peak at  $\Delta_2 = -\Delta_1$  corresponding to cavity induced two-mode two-photon emission disappear as which-path-information gets imprinted on phonon bath. In Fig.5, for negative values of  $\Delta_2$ , similar to Fig.3, the probability  $P_{20}$  dominates. When the detuning  $\Delta_2$  increases  $P_{02}$  and  $P_{11}$  increase and  $P_{02}$  dominates for  $\Delta_2 = 0$  which decreases upto  $\Delta_2 = \Delta_1$  where  $P_{20}$  also has a minima and  $P_{11}$  has a peak corresponding to phonon assisted two-mode two-photon resonance. From above discussions, we find that when detunings from first cavity mode and second cavity mode  $\Delta_1$  and  $\Delta_2$  both are negative the probabilities of single mode two-photon transition and two-mode two-photon transition remain small. However, when both  $\Delta_1$  and  $\Delta_2$  are positive single mode two-photon transition and two-mode two-photon transitions are dominating. Further for  $\Delta_1 = \Delta_2$  two-mode two-photon transition has dominating resonance. Since these two-photon transitions are facilitated by phonons, on increasing temperature the transition probabilities increase. For higher temperatures

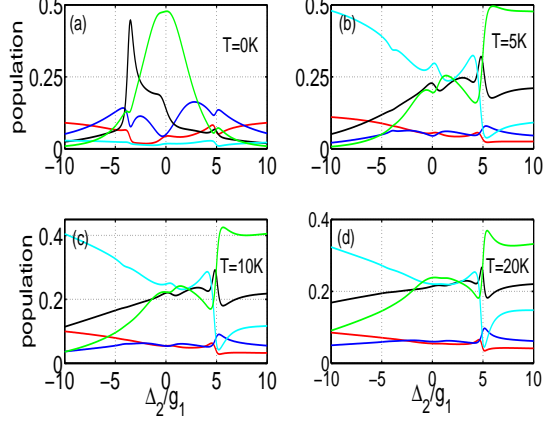


FIG. 3: Photon emission probabilities from the cavity modes,  $P_{10}$  from state  $|g_1, e_2, 1, 0\rangle$  (red line),  $P_{01}$  from state  $|g_1, e_2, 0, 1\rangle$  (blue line),  $P_{20}$  from state  $|g_1, g_2, 2, 0\rangle$  (cyan line),  $P_{02}$  from state  $|g_1, g_2, 0, 2\rangle$  (green line),  $P_{11}$  from state  $|g_1, g_2, 1, 1\rangle$  (black line). The parameters are same as in Fig.2 except  $\Delta_1 = 5g_1\langle B\rangle$ .

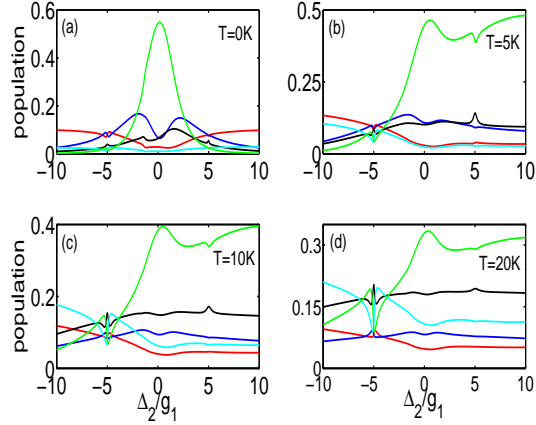


FIG. 4: Photon emission probabilities from the cavity modes,  $P_{10}$  from state  $|g_1, e_2, 1, 0\rangle$  (red line),  $P_{01}$  from state  $|g_1, e_2, 0, 1\rangle$  (blue line),  $P_{20}$  from from state  $|g_1, g_2, 2, 0\rangle$  (cyan line),  $P_{02}$  from state  $|g_1, g_2, 0, 2\rangle$  (green line),  $P_{11}$  from state  $|g_1, g_2, 1, 1\rangle$  (black line). The parameters are  $g_2 = g_1$ ,  $\Delta_1 = -5g_1\langle B\rangle$ ,  $\kappa_1 = \kappa_2 = 0.1g_1$ ,  $\gamma_1 = \gamma_2 = \gamma'_1 = \gamma'_2 = 0.01g_1$ .

two-mode two-photon transition becomes almost independent of detuning  $\Delta_2$  except at resonance  $\Delta_1 = \Delta_2$  which reflects the fact that at higher temperatures the transitions facilitated by phonon absorption or emission are almost equally probable.

In Fig.6, we present calculated spectrum of the cavity modes  $S_i(\omega) = \int_0^\infty dt \int_0^\infty d\tau \langle a_i^\dagger(t)a_i(t+\tau) \rangle \exp i\omega\tau$  for  $i = 1, 2$ . The two time correlation  $\langle a_i^\dagger(t)a_i(t+\tau) \rangle$  are calculated using quantum regression theorem. We plot spectrum at different phonon bath temperatures  $T = 0K$ ,  $T = 5K$ ,  $T = 10K$  and  $T = 20K$ . In order to accommodate four subplots for different temperatures, we normalize the spectrum by dividing all values by its maximum value. The emitted spectrum from cavity modes can be accurately understood using dressed states in excitation manifold (number of excitons in QDs plus number of photons in cavity modes). There could be eight dressed states in two-excitation manifold which are superpositions of  $|e_1, e_2, 0, 0\rangle$ ,  $|e_1, g_2, 1, 0\rangle$ ,  $|e_1, g_2, 0, 1\rangle$ ,  $|g_1, e_2, 1, 0\rangle$ ,  $|g_1, e_2, 0, 1\rangle$ ,  $|g_1, g_2, 2, 0\rangle$ ,  $|g_1, g_2, 0, 2\rangle$ , and  $|g_1, g_2, 1, 1\rangle$ . Two-excitation dressed state decay to four possible dressed states of single excitation manifold, which are superposition of  $|e_1, g_2, 0, 0\rangle$ ,  $|g_1, e_2, 0, 0\rangle$ ,  $|g_1, g_2, 1, 0\rangle$ , and  $|g_1, g_2, 0, 1\rangle$ . The dressed states of single excitation manifold finally decay to  $|g_1, g_2, 0, 0\rangle$ . Therefore theoretically the spectrum of generated photon pair can have as many as 36 peaks. However, for far off-resonant QDs and parameters used in our paper the emission of photons mainly occurs at exciton resonance frequencies and cavity mode frequencies with Stark energy shifts. In Fig.6(a), we plot spectrum of emitted photons from cavity modes using parameters same as in Fig.2 for  $\Delta_2 = 3.5g_1\langle B\rangle$  where cavity induced two-mode two-photon resonance appears. For  $\Delta_2 = 3.5g_1\langle B\rangle$ , the emission

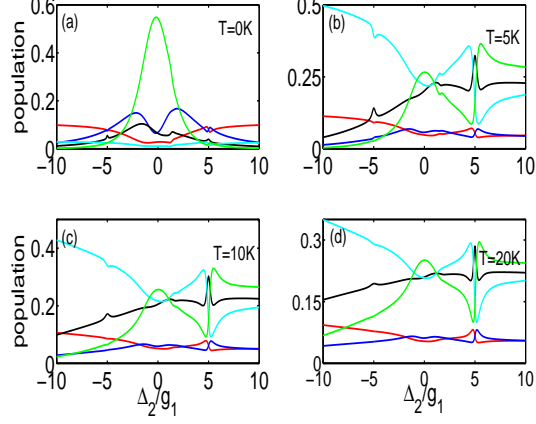


FIG. 5: Photon emission probabilities from the cavity modes,  $P_{10}$  from state  $|g_1, e_2, 1, 0\rangle$  (red line),  $P_{01}$  from state  $|g_1, e_2, 0, 1\rangle$  (blue line),  $P_{20}$  from state  $|g_1, g_2, 2, 0\rangle$  (cyan line),  $P_{02}$  from state  $|g_1, g_2, 0, 2\rangle$  (green line),  $P_{11}$  from state  $|g_1, g_2, 1, 1\rangle$  (black line). The parameters are same as in Fig.4 except  $\Delta_1 = 5g_1\langle B\rangle$ .

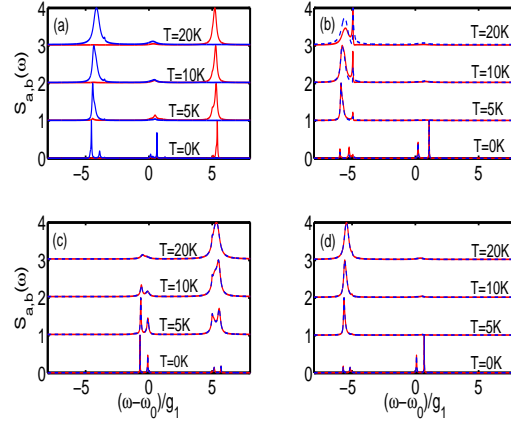


FIG. 6: The spectrum of emitted photons from cavity modes for  $\kappa_1 = \kappa_2 = 0.1g_1$ ,  $\gamma_1 = \gamma_2 = \gamma'_1 = \gamma'_2 = 0.01g_1$ . The red line represents the photon emission from first cavity mode and blue line represents the photon emission from second cavity mode. The parameters are, in (a)  $g_2 = 1.5g_1$ ,  $\Delta_1 = -5g_1\langle B\rangle$ , and  $\Delta_2 = 3.5g_1\langle B\rangle$ , in (b)  $g_2 = 1.5g_1$ ,  $\Delta_1 = 5g_1\langle B\rangle$ , and  $\Delta_2 = 4.8g_1\langle B\rangle$ , in (c)  $g_2 = g_1$ ,  $\Delta_1 = \Delta_2 = -5g_1\langle B\rangle$ , in (d)  $g_2 = g_1$ ,  $\Delta_1 = \Delta_2 = 5g_1\langle B\rangle$ .

from state  $|g_1, g_2, 2, 0\rangle$  is negligible. Therefore, first mode has one photon and second mode has two or one photon at most. Since we have assumed both QDs are identical, the emission from first mode is similar to two-QD single photon dressed states which show two peaks one around exciton resonance frequency ( $\omega - \omega_0 \approx 0$ ) and other around cavity mode frequency ( $\omega - \omega_0 \approx -\Delta_1 = 5g_1\langle B\rangle$ ). However, the emission around cavity mode frequency is enhanced due to two-mode cooperative interaction. In the spectrum of second mode four peaks appear, two peaks corresponding to single-photon two-QD dressed states and two peaks corresponding to two-photon two-QD dressed states having larger Stark shifts. When the temperature of phonon bath is increased the emission of photons around exciton resonance decreases and emission around cavity modes increases, indicating phonon-assisted off-resonant cavity mode feeding. In Fig.6(b), the spectrum of the emitted photons for parameters used in Fig.3 and detuning  $\Delta_2 = 4.8g_1\langle B\rangle$  corresponding to phonon-assisted two-mode two-photon resonance, is shown. At  $T = 0K$ , off-resonant cavity mode interactions are weak, the emission of photons appears mainly around Stark shifted exciton resonance frequencies. For  $\Delta_2 = 4.8g_1\langle B\rangle$  and  $g_2 = 1.5g_1$  spectrum of both modes becomes degenerate. The cavity modes can have one or two photons therefore the spectrum can have four peaks corresponding to emission from one photon two-QD dressed states and two-photon two-QD dressed states. When temperature of phonon bath is raised the interaction with off-resonant cavity modes enhance and the photons are emitted around cavity mode frequencies. However due to Stark shifts emission from states  $|g_1, g_2, 2, 0\rangle$  and  $|g_1, g_2, 0, 2\rangle$  become degenerate, but emission from  $|g_1, g_2, 1, 1\rangle$  exhibits one additional sharp peak. In Fig.6(c) and (d), we plot spectrum using parameters of Figs.4 and 5, for  $\Delta_1 = \Delta_2$  corresponding to phonon-

assisted two-mode two-photon resonance. At  $T = 0K$ , we get emission around one photon and two-photon Stark shifted exciton resonance frequency as off-resonant cavity interactions are weak. When temperature of the phonon bath is increased more and more photons are emitted around cavity modes indicating phonon assisted off-resonant cavity mode feeding and enhanced two-photon transitions. Further for positive detunings the phonon-assisted two-photon interactions are stronger than for negative detunings the spectrum exhibits single peak around cavity mode frequencies.

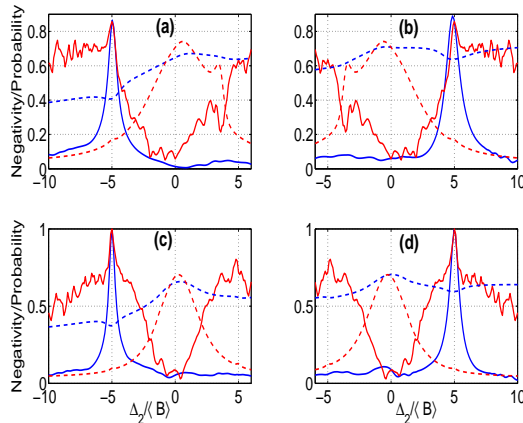


FIG. 7: The probability of generation (dashed line) and the negativity (solid line) of entangled two-photon state emitted through two modes at phonon bath temperatures  $T = 0K$  (red color) and  $T = 10K$  (blue color), using parameters, in (a) same as in Fig.2, in (b) same as in Fig.3, in (c) same as in Fig.4, and in (d) same as in Fig.5.

#### IV. ENTANGLEMENT BETWEEN TWO MODES

When both photons are emitted from cavity modes, the number of photons emitted from each mode form the basis of a qutrit<sup>32</sup>. The state of the emitted photons at time  $t$  can be described as

$$|\psi(t, \tau)\rangle \sim \{a_1^\dagger(t)a_1^\dagger(t+\tau) + a_1^\dagger(t)a_2^\dagger(t+\tau) + a_2^\dagger(t)a_2^\dagger(t+\tau)\}|0, 0\rangle, \quad (14)$$

where  $\tau$  is delay time between photons and state  $|0, 0\rangle$  is two mode vacuum state. In order to quantitatively measure the entanglement between two modes, we calculate negativity for the entangled state of emitted photons. The negativity is defined as the absolute value of the sum of the negative eigenvalues of the partially transposed density matrix<sup>33</sup>. The negativity for the state (14) is given by

$$\mathcal{N} = \frac{|\rho_{20,11}| + |\rho_{20,02}| + |\rho_{11,02}|}{|\rho_{20,20}| + |\rho_{02,02}| + |\rho_{11,11}|} \quad (15)$$

where  $\rho_{ij,kl}$  is density matrix element for emitted two photons through two modes. To reconstruct the density matrix of photons emitted from the cavity modes, coincidence measurements are performed. The photon coincidence measurements are given by two time correlation functions  $G_{ij,kl}^2(t, \tau) = \langle a_i^\dagger(t)a_j^\dagger(t+\tau)a_k(t+\tau)a_l(t) \rangle$ , where  $t, \tau$  are time of arrival of first photon at detector, delay time for second photon, indices  $i, j, k, l$  are corresponding to the mode from which photon is emitted. If both photons are emitted from same cavity mode  $i = j$  ( $k = l$ ). The reconstructed density matrix elements can be written as  $\rho_{20,11} \propto \int_0^\infty dt \int_{-\infty}^\infty d\tau G_{11,12}^2(t, \tau)$ ,  $\rho_{20,02} \propto \int_0^\infty dt \int_{-\infty}^\infty d\tau G_{11,22}^2(t, \tau)$ ,  $\rho_{11,02} \propto \int_0^\infty dt \int_{-\infty}^\infty d\tau G_{12,22}^2(t, \tau)$ ,  $\rho_{20,20} \propto \int_0^\infty dt \int_{-\infty}^\infty d\tau G_{11,11}^2(t, \tau)$ ,  $\rho_{02,02} \propto \int_0^\infty dt \int_{-\infty}^\infty d\tau G_{22,22}^2(t, \tau)$ , and  $\rho_{11,11} \propto \int_0^\infty dt \int_{-\infty}^\infty d\tau G_{12,21}^2(t, \tau)$ <sup>34</sup>. We calculate probability of generating entangled two-qutrit state and negativity corresponding to the parameters used in Figs.2, 3, 4, and 5 at phonon bath temperatures  $T = 0K$  and  $T = 10K$ . We find in the absence of phonon interaction at  $T = 0K$ , the probability of generating two entangled qutrits (red dashed line), is maximum around  $\Delta_2 = 0$  where generation of two-photon state  $|g_1, g_2, 0, 2\rangle$  dominates and gradually decreases on increasing  $|\Delta_2|$ . In the case of asymmetric dipole couplings  $g_1 \neq g_2$ , shown in Fig.7(a) and (b), at cavity induced two-photon two-mode resonance it also has larger value where generation of two-photon state  $|g_1, g_2, 1, 1\rangle$  dominates.

The maximum probability of generating entangled qutrits remains around 0.7 due to losses from spontaneous decay of one or both excitons and photon emission from states  $|e_1, g_2, 1, 0\rangle$ ,  $|e_1, g_2, 0, 1\rangle$ ,  $|g_1, e_2, 1, 0\rangle$ , and  $|g_1, e_2, 0, 1\rangle$ . The negativity (red solid line) on the other hand is maximum for  $\Delta_1 = \Delta_2$  when emitted photons match in frequencies. It is clear that the probability of generating entangled two-qutrit is negligible when negativity is maximum in the absence of phonon interactions. We show probability of generating entangled two-qutrit states and negativity after including phonon interaction at  $T = 10K$  with blue dashed and solid lines, respectively. We find that photons are maximally entangled for  $g_1 = g_2$  and  $\Delta_1 = \Delta_2$ , and negativity drops to zero for  $\Delta_2 \neq \Delta_1$ , since which-path information is revealed by the phonons involved in facilitating off-resonant transitions when cavity modes have different detunings. Further for  $g_1 = g_2$  the spectrum of emitted photons from both modes overlap perfectly which makes both modes maximally entangled. The probability of generating two-qutrit entangled state is larger than 0.6 for positive detunings and is smaller than 0.4 for negative detunings because of asymmetric nature of phonon induced two-mode two-photon interactions. Therefore, for parameters used in Fig.3 and Fig.5, one can generate highly entangled two-mode two-photon state using phonon-assisted two-mode two-photon interactions.

## V. CONCLUSIONS

We have predicted large phonon-assisted two-mode two-photon interactions in the system of two off-resonantly coupled QDs inside a bimodal photonic crystal cavity. We have found that the cavity field induced two-mode two-photon resonances, which appear for  $g_1 \neq g_2$ , are completely wiped out in the presence of exciton-phonon interactions and the phonon-assisted two-mode two-photon resonances occur at  $\Delta_1 = \Delta_2$ . Further, these interactions are more pronounced for positive detunings. Our results could open up a new route for generating entangled states of photons from chip-based QD-cavity systems.

## VI. ACKNOWLEDGEMENTS

This work was supported by DST SERB Fast track young scientist scheme SR/FTP/PS-122/2011.

- 
- <sup>1</sup> A. Kiraz, C. Reese, B. Gayral, L. Zhang, W. V. Schoenfeld, B. D. Gerardot, P. M. Petroff, E. L. Hu, and A. Imamoglu, *J. Opt. B: Quantum Semiclass. Opt.*, **5**, 129 (2003); Jelena Vučković, and Y. Yamamoto, *Appl. Phys. Lett.* **82**, 2374 (2003).
  - <sup>2</sup> A. Faraon, A. Majumdar, D. Englund, E. Kim, M. Bajcsy, and J. Vučković, *New J. Phys.* **13**, 055025 (2011); S. Sun, H. Kim, Z. Luo, G. S. Solomon, and E. Waks, *Science* **361** (6397), 57 (2018); H.-R. Wei and F.-G. Deng, *Scientific Reports* **4**, 7551 (2014); M. Davanco, J. Liu, L. Sapienza, C.-Z. Zhang, J. Vinícius De M. Cardoso, V. Verma, R. Mirin, S. W. Nam, L. Liu, and K. Srinivasan, *Nature Communications* **8**, 889 (2017).
  - <sup>3</sup> F. Liu, A. J. Brash, J. O'Hara, Luis M. P. P. Martins, C. L. Phillips, R. J. Coles, B. Royall, E. Clarke, C. Bentham, N. Prtljaga, I. E. Itskevich, L. R. Wilson, M. S. Skolnick, and A. Mark Fox, *Nature Nanotechnology* **13**, 835 (2018); M. D. Birowosuto, H. Sumikura, S. Matsuo, H. Taniyama, P. J. van Veldhoven, R. Nötzel, and M. Notomi, *Scientific Reports* **2**, 321 (2012).
  - <sup>4</sup> G. Khitrova, H. M. Gibbs, M. Kira, S. W. Koch, and A. Scherer, *Nature Physics* **2**, 81 (2006); T. Yoshie, A. Scherer, J. Hendrickson, G. Khitrova, H. M. Gibbs, G. Rupper, C. Ell, O. B. Shchekin, and D. G. Deppe, *Nature* **432**, 200 (2004); Y. Ota, D. Takamiya, R. Ohta, H. Takagi, N. Kumagai, S. Iwamoto, and Y. Arakawa, *Appl. Phys. Lett.* **112**, 093101 (2018); Y. Ota, R. Ohta, N. Kumagai, S. Iwamoto, and Y. Arakawa, *Phys. Rev. Lett.* **114**, 143603 (2015).
  - <sup>5</sup> T. H. Stievater, X. Li, D. G. Steel, D. Gammon, D. S. Katzer, D. Park, C. Piermarocchi, and L. J. Sham, *Phys. Rev. Lett.* **87**, 133603; K. Kuruma, Y. Ota, M. Kakuda, S. Iwamoto, and Y. Arakawa, *Phys. Rev. B* **97**, 235448 (2018).
  - <sup>6</sup> A. Majumdar, E. D. Kim, Y. Gong, M. Bajcsy, and J. Vučković, *Phys. Rev. B* **84**, 085309 (2011); C. Roy and S. Hughes, *Phys. Rev. Lett.* **106**, 247403 (2011).
  - <sup>7</sup> N. Akopian, N. H. Lindner, E. Poem, Y. Berlatzky, J. Avron, D. Gershoni, B. D. Gerardot and P. M. Petroff, *Phys. Rev. Lett.* **96**, 130501 (2006).
  - <sup>8</sup> M. Müller, S. Bounouar, K. D. Jns, M. Glässl, and P. Michler, *Nature Photonics* **8**, 224 (2014).
  - <sup>9</sup> A. Dousse, J. Suffczynski, A. Beveratos, O. Krebs, A. Lemaitre, I. Sagnes, J. Bloch, P. Voisin and P. Senellart, *Nature* **466**, 217 (2010).
  - <sup>10</sup> H. Wang, H. Hu, T.-H. Chung, J. Qin, X. Yang, J.-P. Li, R.-Z. Liu, H.-S. Zhong, Y.-M. He, X. Ding, Y.-H. Deng, Q. Dai, Y.-H. Huo, S. Höfling, C.-Yang Lu, and J.-Wei Pan, *Phys. Rev. Lett.* **122**, 113602 (2019).
  - <sup>11</sup> X. Ding, Y. He, Z.-C. Duan, N. Gregersen, M.-C. Chen, S. Unsleber, S. Maier, C. Schneider, M. Kamp, S. Höfling, C.-Y. Lu, and J.-W. Pan, *Phys. Rev. Lett.* **116**, 020401 (2016); P. K. Pathak and S. Hughes, *Phys. Rev. B* **82**, 045308 (2010).
  - <sup>12</sup> P. Kaer, T. R. Nielsen, P. Lodahl, A.-P. Jauho, and J. Mørk, *Phys. Rev. B* **86**, 085302 (2012).
  - <sup>13</sup> A. Nazir and D. P S McCutcheon, *J. Phys.: Condens. Matter* **28**, 103002 (2016).

- <sup>14</sup> A. Laucht, N. Hauke, J. M. Villas-Bôas, F. Hofbauer, G. Böhm, M. Kaniber, and J. J. Finley, *Phys. Rev. Lett.* **103**, 087405 (2009). Y. Ota, S. Iwamoto, N. Kumagai, and Y. Arakawa, *Phys. Rev. Lett.* **107**, 233602 (2011).
- <sup>15</sup> D. Englund, A. Majumdar, A. Faraon, M. Toishi, N. Stoltz, P. Petroff, and Jelena Vučković, *Phys. Rev. Lett.* **104**, 073904 (2010); S. Ates, S. M. Ulrich, A. Ulhaq, S. Reitzenstein, A. Löffler, S. Hofling, A. Forchel, and P. Michler, *Nat. Photon.* **3**, 724 (2009); A. J. Bennett, J. P. Lee, D. J. P. Ellis, T. Meany, E. Murray, F. F. Floether, J. P. Griffiths, I. Farrer, D. A. Ritchie, A. J. Shields, *Sci. Adv.* **2**, e1501256 (2016); E. B. Flagg, A. Müller, S. V. Polyakov, A. Ling, A. Migdall, and G. S. Solomon, *Phys. Rev. Lett.* **104**, 137401 (2010).
- <sup>16</sup> S. Weiler, A. Ulhaq, S. M. Ulrich, D. Richter, M. Jetter, P. Michler, C. Roy, and S. Hughes, *Phys. Rev. B* **86**, 241304(R) (2012); R. Oulton, J. J. Finley, A. I. Tartakovskii, D. J. Mowbray, M. S. Skolnick, M. Hopkinson, A. Vasanelli, R. Ferreira, and G. Bastard *Phys. Rev. B* **68**, 235301 (2003).
- <sup>17</sup> Y.-Shan Lee and S.-Di Lin, *Optics Letters* **39**, 23 (2014); M. Kaniber, A. Laucht, A. Neumann, J. M. Villas-Bas, M. Bichler, M.-C. Amann, and J. J. Finley, *Phys. Rev. B* **77**, 161303(R) (2008).
- <sup>18</sup> A. Majumdar, M. Bajcsy, A. Rundquist, E. Kim, and J. Vučković *Phys. Rev. B* **85** 195301 (2012).
- <sup>19</sup> M. Calic, C. Jarlov, P. Gallo, B. Dwir, A. Rudra, and E. Kapon, *Scientific Reports* **7**, 4100 (2017).
- <sup>20</sup> J. K. Verma, Harmanpreet Singh, and P. K. Pathak, *Phys. Rev. B* **98**, 125305 (2018).
- <sup>21</sup> J. K. Verma, Harmanpreet Singh, and P. K. Pathak, *J. Opt. Soc. Am. B* **36**, 1200-1207 (2019).
- <sup>22</sup> M. Glässl, A. M. Barth, K. Gawarecki, P. Machnikowski, M. D. Croitoru, S. Luker, D. E. Reiter, T. Kuhn, and V. M. Axt, *Phys. Rev. B* **87**, 085303 (2013); S. Bounouar, M. Müller, A. M. Barth, M. Glässl, V. M. Axt, and P. Michler *Phys. Rev. B* **91**, 161302(R) (2015); M. Glässl, A. M. Barth, and V. M. Axt *Phys. Rev. Lett.* **110**, 147401 (2013); A. M. Barth, S. Luker, A. Vagov, D. E. Reiter, T. Kuhn, and V. M. Axt, *Phys. Rev. B* **94**, 045306 (2016).
- <sup>23</sup> J. H. Quilter, A. J. Brash, F. Liu, M. Glässl, A. M. Barth, V. M. Axt, A. J. Ramsay, M. S. Skolnick, and A. M. Fox, *Phys. Rev. Lett.* **114**, 137401 (2015).
- <sup>24</sup> T. Czerniuk, D. Wigger, A. V. Akimov, C. Schneider, M. Kamp, S. Höfling, D. R. Yakovlev, T. Kuhn, D. E. Reiter, and M. Bayer, *Phys. Rev. Lett.* **118**, 133901 (2017).
- <sup>25</sup> K. Kamide, Y. Ota, S. Iwamoto, and Y. Arakawa, *Phys. Rev. A* **96**, 013853 (2017).
- <sup>26</sup> P. K. Pathak and S. Hughes, *Phys. Rev. B* **80**, 155325 (2009).
- <sup>27</sup> I. Wilson-Rae and A. Imamoglu, *Phys. Rev. B* **65**, 235311(2002); D. P. S. McCutcheon and A. Nazir, *New J. Phys.* **12**, 113042 (2010); C. Roy and S. Hughes, *Phys. Rev. X* **1**, 021009 (2011); C. Roy and S. Hughes, *Phys. Rev. Lett.* **106**, 247403(2011).
- <sup>28</sup> H. J. Sniijders, J. A. Frey, J. Norman, H. Flayac, V. Savona, A. C. Gossard, J. E. Bowers, M. P. van Exter, D. Bouwmeester, and W. Löffler, *Phys. Rev. Lett.* **121**, 043601 (2018).
- <sup>29</sup> S. M. Ulrich, S. Ates, S. Reitzenstein, A. Löffler, A. Forchel, and P. Michler *Phys. Rev. Lett.* **106**, 247402 (2011).
- <sup>30</sup> S. M. Tan, *J. Opt. B* **1**, 424 (1999).
- <sup>31</sup> M. Pleinert, J. von Zanthier, and G. S. Agarwal, *Optica* **4**, 779 (2017).
- <sup>32</sup> W. M. Pimenta, B. Marques, T. O. Maciel, R. O. Vianna, A. Delgado, C. Saavedra, and S. Pádua *Phys. Rev. A* **88**, 012112 (2013).
- <sup>33</sup> G. Vidal and R. F. Werner, *Phys. Rev. A* **65**, 032314 (2002).
- <sup>34</sup> F. Troiani, J. I. Perea, and C. Tejedor *Phys. Rev. B* **74**, 235310(2006); G. Pfanner, M. Seliger, and U. Hohenester, *Phys. Rev. B* **78**, 195410 (2008).